20. E. J. Krogstad, thesis, State University of New York, Stony Brook (1988).
21. S. Balakrishnan and V. Rajamani, *J. Geol.* **95**, 219 (1987).
22. C. R. L. Friend, A. P. Nutman, V. R. McGregor, *J. Geol. Soc. London* **144**, 369 (1987).
23. J. Saleeby, *Annu. Rev. Earth Planet. Sci.* **11**, 45 (1983).
24. E. M. Moores, *Science* **234**, 65 (1986).
25. P. Vidal, J. J. Peucat, J. Bernard-Griffiths, K. C. Condie, *Terra Cognita* **8**, 262 (1988).
26. S. A. Drury and R. W. Holt, *Tectonophysics* **65**, T1 (1980).
27. J. Bernard-Griffiths, B. M. Jahn, S. K. Sen, *Precamb. Res.* **37**, 343 (1987).
28. This paper is the result of an Indo-U.S. collaborative project between V. Rajamani and G. N. Hanson supported by NSF grants INT-8205525 and INT-8519507 and NASA grant NAG-985. This manuscript benefited from reviews by K. Mezger, O. Evans, W. D. Sharp, S. McLennan, D. Davis, and two anonymous reviewers.

31 October 1988; accepted 1 February 1989

The Axial Oxygen Atom and Superconductivity in $YBa_2Cu_3O_7$

S. D. CONRADSON AND I. D. RAISTRICK

Changes in the copper K-edge x-ray absorption spectrum of $YBa_2Cu_3O_7$ across the critical temperature indicate that, accompanying the superconducting transition, the mean square relative displacement of some fraction of the Cu2–O4 bonds becomes smaller or more harmonic (or both), that there may be a slight increase in the associated Cu1–O4 distance, and that electronic states involving these atom pairs become more atomic-like. If there is an association between the superconductivity and this lattice instability, then the bridging axial oxygen is of central importance in determining the high transition temperature of $YBa_2Cu_3O_7$. Because this structural perturbation will affect the dynamic polarizability of the copper oxygen sublattice, it is consistent with an excitonic pairing mechanism in these materials.

DESPITE THE INTENSITY WITH which the superconducting cuprates have been studied since their discovery (*1*), direct information about changes in their atomic and electronic structures in the vicinity of the transition temperature is largely lacking, and the mechanism of superconductivity in these materials is still uncertain (*2*). Copper K-edge x-ray absorption spectroscopy (XAS) measurements have shown that chemical modification of $YBa_2Cu_3O_7$ (for example, by doping) results in small differences in the x-ray absorption near-edge structure (XANES) indicative of corresponding changes in structural properties (*3*). Although these differences are quite subtle, we have recently found that they can be amplified by subtracting the XANES of the modified compounds from that of a high-quality, undoped sample (*4*). Features in these difference spectra are easily identified with respect to the assigned transitions in the spectrum of $YBa_2Cu_3O_7$ (*5, 6*) and their magnitudes show a consistent trend with the dopant concentrations. The sensitivity and utility of this difference spectrum approach suggested its application to the examination of the temperature dependence of $YBa_2Cu_3O_7$, as reflected in the XANES. In this paper, we report direct evidence for specific changes in the atomic structure and electronic configuration accompanying the transition to the superconducting state.

We have examined two samples of $YBa_2Cu_3O_7$, prepared from Y_2O_3, $BaCO_3$, and CuO by conventional ceramic procedures. Samples 1 and 2 were both single phase (as determined by x-ray and electron diffraction), both showed superconducting transition temperatures (onset) of 92 K, and they had oxygen stoichiometries of, respectively, 6.97 and 6.98 (thermogravimetric analysis). The superconducting volume fraction (after a demagnetization correction) of sample 1 was 0.97 at 7 K, whereas that of sample 2 was only 0.35. Certain aspects of the diffraction patterns of sample 2 suggested less than perfect order in the *c* direction. The differences in the preparations of these two samples were that sample 1 was fired at 950°C, slowly cooled, and given a long anneal in O_2 at 450°C, whereas sample 2 was fired at 900°C and then furnace-cooled in O_2 to room temperature directly. Amounts of these samples calculated to produce an absorbance of unity over the copper K edge were used for these measurements. All XAS data were recorded at the Stanford Synchrotron Radiation Laboratory on beam line I-5 under dedicated operating conditions (3-GeV electron energy, 50-mA beam current, no positrons). The inflection point of the first feature in the copper metal spectra used for calibration was defined as 8980.3 eV. The effects of background variations on the normalized difference spectra were compensated for by performing small (0 to 0.7%) adjustments to maximize the overlap of the two spectra from 8980 to 8982 and 9023 to 9030 eV.

The XANES spectrum of sample 1 is shown in Fig. 1. Below the ionization threshold at around 9000 eV, features in the XANES labeled A to E (*5, 6*) correspond to transitions from the core level of the absorbing atom to the bound, localized electronic states of the system (*5–11*). Above the ionization threshold, the XANES contains discrete transitions to more delocalized and multiple-scattering types of final states in addition to the low *k* region of the extended x-ray absorption fine structure (EXAFS). The energies and intensities of these types of resonances, originating in the interaction of the low kinetic energy photoelectron with the potential of the neighboring atoms, are very sensitive to the exact structure of the local cluster around the absorbing atom (*7, 9*). This XANES spectrum, extending about 50 eV above the onset of absorption, therefore simultaneously probes both the electronic states of the copper atoms and the atomic structure around them.

Difference spectra have been computed for sample 1 for five pairs of temperatures up to 150 K (Fig. 2). In addition to changes in the intensities of the localized transitions A, B, C, and D, a pattern of oscillations with extrema at 9000, 9003, 9006, 9010, 9014, and 9020 eV is evident in the structure-sensitive region. The iteration of this pattern and the virtually identical shapes of the spectra obtained for samples 1 and 2 across the transition temperature T_c indicate that these spectra reflect the same distinct lattice instability. This spectral pattern was not

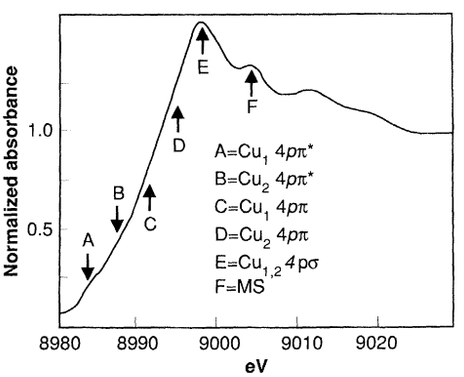

Fig. 1. The Cu K XANES of $YBa_2Cu_3O_7$ at 11 K. Transitions to discrete, localized final states are indicated by arrows and assigned based on (*5*), MS = multiple scattering-type transition. Alternative assignments are discussed in (*16*). Features corresponding to some of these transitions are more difficult to see in this powder spectrum than in those from oriented samples or in the difference spectra.

Electronics Research and Isotope and Structural Chemistry Groups, Los Alamos National Laboratory, Los Alamos, NM 87545.

found for a tetragonal material with an oxygen stoichiometry close to six, and is therefore indicative of a structural perturbation specific to the orthorhombic phase. The differences in the absorption are only of the order of 1% of that of the transition to the continuum, indicating that this perturbation is subtle, or occurs within only a fraction of the unit cells at any instant, or both. If the perturbation was due to an impurity phase (which can only be present at <1% level, as shown by the XRD and flux exclusion data), then there would undoubtedly be a large shift in energy of the XANES features as well as the observed change in absorption (*12*). Because the subtractions did not produce the derivative-like spectra that result from shifts as small as a few tenths of an electron volt, this modification of the structure must be occurring in the bulk, superconducting phase. It is therefore especially notable that, relative to the spectra at higher and lower temperatures, the direction of the

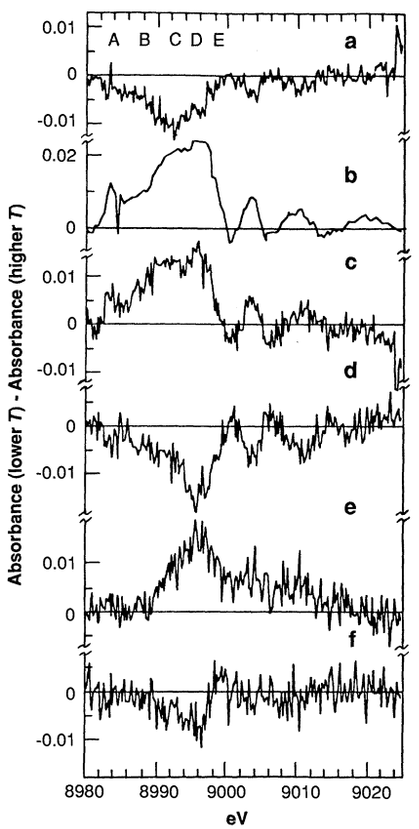

Fig. 2. $YBa_2Cu_3O_7$ Cu K-edge XANES difference spectra as a function of the higher temperature spectra subtracted from the lower. The temperatures of the sample from which the spectra were generated are as follows: (**a**) 11 to 90 K; (**b**) sample 2, 87 to 105 K; (**c**) 90 to 95 K; (**d**) 95 to 105 K; (**e**) 105 to 120 K; (**f**) 120 to 150 K. All spectra are from sample 1 except as noted. A through E are at the same energies as in Fig. 1, making apparent the correspondence of the features in the difference spectra with those in the XANES.

changes reverses as T_c is crossed. These differences, therefore, do not originate in a simple thermal effect but reflect a distinct process associated with the onset of superconductivity.

Additional information about this structural perturbation can be obtained from the EXAFS, where data from sample 2 show an observable temperature dependence (Fig. 3a). These differences, first evident at $k = 9$ Å^{-1}, increase with increasing energy, suggesting that the dominant effect is a change in the Debye-Waller factor, which has an exponential energy dependence. This suggestion is corroborated by curve-fitting results and is seen in the Fourier transforms of the EXAFS (Fig. 3b). The difference in the transform around $R = 2$ Å is caused by the contribution of the Cu2–O4 pair, which is large at the lower temperature but undetectably small relative to the contributions of the other neighboring atoms above T_c (*13*). The increased contribution of this atom pair to the EXAFS just below T_c almost certainly results from an increase in the harmonic character of the Cu2–O4 mean square relative displacement (MSRD), or a decrease in its amplitude, or both. The Cu2–O4 distance at 87 K is, within ±0.01 to 0.03 Å, the same as that determined crystallographically (*14, 15*). (The difference in the transform around $R = 4$ Å probably reflects a change in the contributions of the Cu1–Cu2 pair, which would be affected by multiple scattering through O4.)

Changes with temperature in the EXAFS of sample 1 are below the detectability limit of the analysis. This is in agreement with the smaller amplitude of the XANES difference spectra for sample 1 relative to sample 2. The larger magnitude of the change for sample 2 may result from its lower temperature at 87 K instead of 90 K, which could be significant because of the proximity to T_c. Even if this temperature difference is not the reason that the spectrum of sample 2 is larger, the fact that the magnitudes of the effect are greater for the sample with the smaller superconducting volume fraction does not imply that the structural perturbations observed here are unrelated to the superconductivity. The exact nature of the static structural difference between samples 1 and 2 is unknown, but the XAS data indicate that the copper-oxygen sublattice is not severely affected (*13*). It is quite possible that the additional structural disorder evident in sample 2 increases the temperature dependence of the MSRDs, while simultaneously disrupting carrier pairing in affected regions of the crystal. Regardless of the origin of the difference between the samples, the similarity in the difference spectra demonstrates that the change in the Cu2–O4 MSRD across T_c in sample 2 also accompanies the superconducting transition in sample 1, which is almost 100% superconducting.

The behavior of the transitions to localized final states (<9000 eV) is completely consistent with this interpretation of the EXAFS. In addition, these transitions exhibit some unique characteristics. The principal features in this region of the difference spectra correspond to changes in the intensity of transitions C and D (Fig. 2). Transition D always changes in the same direction as the feature at 9003 eV and its intensity is always about twice that of the difference between the 9003 and 9000 eV extrema. It thus appears to be directly correlated with the structural change discussed above. The difference in the intensity of transition C, although always in the same direction as D, becomes significant only just above T_c, becomes large just below this temperature, and continues to increase in magnitude until it is the largest feature in the 11 to 90 K difference spectrum (Fig. 2a).

The results of Heald *et al.* (*5*) and Kosugi *et al.* (*6*) on oriented samples indicate that C and D originate in transitions from, respectively, the Cu1 and Cu2 1*s* initial states to final states possessing Cu1 $4p_x\pi$ and Cu2 $4p_z\pi$ character (*16*). An increase in the intensities of these transitions is caused by a decrease in the overlap (*8*) of the Cu1 $4p_x$ and Cu2 $4p_z$ orbitals with those nearby oxygen orbitals of the appropriate orientations and energies. In other words, the character of these final states becomes more atomic-like with the onset of superconductivity. The most important Cu1–O interaction is likely to be the overlap of O4 p_x with Cu1 $4p_x$, because O4 is 0.1 Å closer to Cu1 than O1 (*14, 15*). We believe that the most important Cu2–O interaction is the σ-type overlap of the O4 $3p_z$ with the Cu2 $4p_z$ rather than the π-type overlap with the O2,3. If this were not the case, any perturbation of the Cu2–O2,3 bonding which affected transition D would also have produced an observable effect on E (the Cu2 $4p\sigma \leftarrow 1s$ transition), which possesses the largest amplitude of all of the transitions in the XANES (*5, 6*).

Intensity increases in transition D are therefore understandable in terms of a reduction in the vibronically driven overlap of the Cu2 $4p_z$ orbital with the O4 p_z as the Cu2–O4 MSRD becomes smaller or more harmonic (or both) and the vibronic excursion of O4 toward Cu2 diminishes. The increase in the amplitude of transition C must result from a similar decrease in overlap, in this case between the Cu1 $4p_x$ and O4 p_x orbitals. Because the Cu1–O4 bond is short, an increase in static bond length is necessarily implied. The EXAFS of sample

2, referred to above, does show evidence of a 0.02 to 0.03 Å increase in the Cu1–O4 distance when analyzed with highly constrained curve fits (*13*). This change is within the sensitivity level of the analysis as determined from related materials. As expected for this interpretation, thermal contraction at temperatures well removed from T_c reduces the intensities of both transitions. The small displacement of the O4 atom, its coupling to the thermal and static disorder, and the restriction of these structural fluctuations to a very limited range around T_c would account for the failure to observe this specific perturbation by other methods (*14, 17, 18*), including EXAFS analysis (*19*).

The transitions to copper 4*p* states, probed by the copper K-edge XANES, are very much higher in energy than the states close to the Fermi level that are involved in the superconductivity. Nevertheless, the electronic perturbations discussed above will have counterparts in those low-energy states that overlap spatially with the affected Cu1 $4p_x$, Cu2 $4p_z$, O4 $3p_z$, and O4 $3p_x$ orbitals. These are the same low-energy states responsible for fine structure in the density of states near the Fermi level, which may greatly enhance the sensitivity of $YBa_2Cu_3O_7$ to

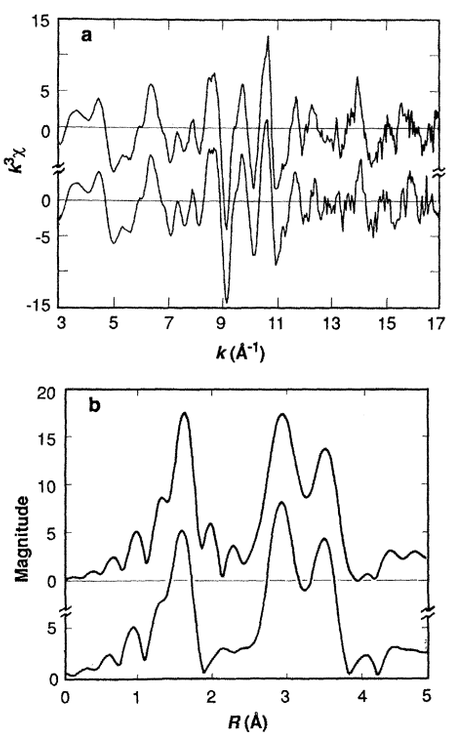

Fig. 3. The Cu K-edge EXAFS (**a**) and the corresponding Fourier transform moduli (**b**) of sample 2 at 87 K (lower curve) and 105 K (upper curve). The feature near R = 2.0 Å in the 105 K spectrum is actually a side lobe, which is canceled out when the contribution of the Cu2–O4 shell at 2.3 Å becomes significant as the temperature is lowered to 87 K (see text).

structural and chemical modifications (*20, 21*).

Our data are evidence for a perturbation in the atomic and electronic structure in the vicinity of T_c (Fig. 4) that centers on the O4 atoms, the bridge between the current-carrying CuO_2 planes and the CuO_3 chains. A lattice fluctuation near T_c has previously been proposed on the basis of ultrasound measurements (*22*) and other EXAFS experiments (*23*). Heat capacity measurements made at very slow scan rates have shown a first-order transition 3.65 K above the feature associated with zero resistance (*24*), and other measurements have suggested related small, sample preparation and treatment-dependent specific heat fluctuations just above T_c (*24, 25*). These results can be compared with the fluctuations in the XANES between 95 and 150 K and could be accounted for if the modification of the Cu2–O4 MSRD was cooperative, which would not be unexpected for this type of perturbation. A growing body of experimental evidence also suggests that O4 play a critical role in the superconductivity of $YBa_2Cu_3O_7$. Infrared photoinduced absorption measurements have recently shown that photo-induced carriers are coupled to the Cu2–O4 vibration (*26*). Cava *et al.* have demonstrated that the relationship between T_c and δ in $YBa_2Cu_3O_{7-\delta}$ is directly correlated with the Cu2–O4 bond length (*17*). In addition, magnetic resonance (*18*), electron energy loss spectroscopy (EELS) (*27*), and Cu L_3 XANES (*28*) indicate that O4 is the location of those doping-induced holes that do not reside in the CuO_2 planes and may be important as described below. Based on our XANES results, we can now suggest a relationship between instability, the role of O4 in determining the electronic properties, and superconductivity in $YBa_2Cu_3O_7$.

The increase in harmonic character or decrease in the amplitude of the Cu2–O4 MSRD (or both) and the increase in the Cu1–O4 distance at those sites at which it occurs should lower the electron-phonon coupling parameter of the Cu1,2–O4 bonds (*29*). The displacement would be coupled to the transfer of electron density as shown in Fig. 4. In addition, it has been suggested that a low-energy, Cu^{2+}–$O^- \leftrightarrow Cu^{3+}$–$O^{2-}$, excitation provides the intrinsic pairing force in the planes (*30*). Although the holes in the chains are not thought to play a significant carrier role, those centered on O4 could provide a source of charge transfer-coupled dynamic polarizibility directed along the O4–Cu1–O4 axis (*30–32*). The magnitude of the pairing attraction in the CuO_2 planes produced by charge transfer to or from O4 would considerably exceed that resulting from nuclear motion or induced dipole types of responses. Pair formation would therefore be facilitated by an enhancement of the oscillator strength of this charge transfer excitation, which should be strongly coupled to the changes at O4 we have described. In addition, the greater localization of the holes residing on the O4 atom (a consequence of the increase in the atomic character of the states in which they reside) will decrease their mobility, driving the pairing in the planes still further. The change in the Cu2–O4 MSRD may also be coupled to the Jahn-Teller modes and consequently the phononic excitations within the planes, and increase the coupling between the interplane charge transfer fluctuations and structural degrees of freedom (*32*).

Without attempting to distinguish whether the lattice instability we have observed is coupled directly to the formation of Cooper pairs or whether it is a precursor that facilitates the pair formation mechanism, it is apparent that the perturbation of the Cu2–O4–Cu1 moiety provides models for an excitonic basis for superconductivity in $YBa_2Cu_3O_7$. The experimental support for this mechanism has recently been reviewed by Little (*33*), its original proponent (*34*). In one variant of this model (*32*), pair formation in the CuO_2 planes is strengthened by coupling to dynamic electron transfer between these axial oxygen atoms and the atoms within an adjacent, polarizable layer. A lattice instability at or just above T_c

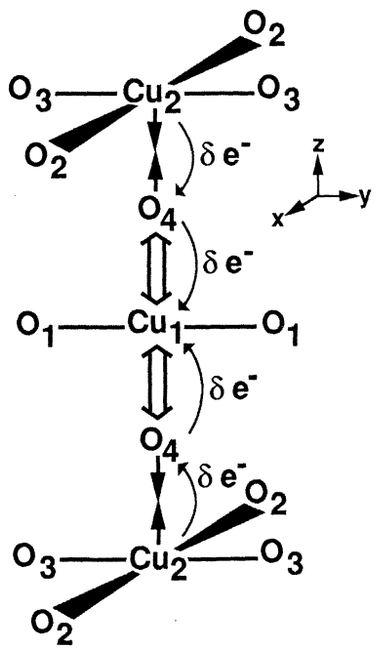

Fig. 4. Model for the changes in structure and charge density accompanying the superconducting transition in the Cu_3O_{12} cluster. Filled arrows indicate bonds whose MSRD becomes smaller, or more harmonic, or both; empty arrows indicate bonds that may become longer.

that results in an increase in the oscillator strength of these excitations, such as we have observed, could then turn on the superconducting phase transition. Even if the mechanism is primarily phonon-mediated, an anharmonic mode such as that described here could have a much reduced isotope effect on T_c than that expected from standard Bardeen-Cooper-Schrieffer phenomenology (*29*), as is found for $YBa_2Cu_3O_7$ (*35*). This same mechanism could be operative in the other cuprate-based, axial oxygen-containing superconductors, and especially in the thallium- and bismuth-based compounds, where these oxygen atoms are also the bridge between the CuO_2 planes and a highly polarizable layer.

REFERENCES AND NOTES

1. J. G. Bednorz and K. A. Müller, *Z. Phys. B* **64**, 189 (1986); M. K. Wu *et al.*, *Phys. Rev. Lett.* **58**, 908 (1987); C. C. Torardi *et al.*, *Science* **240**, 631 (1988); M. A. Subramanian *et al.*, *Nature* **332**, 420 (1988); S. S. P. Parkin *et al.*, *Phys. Rev. Lett.* **61**, 750 (1988).
2. T. M. Rice, *Z. Phys. B* **67**, 141 (1987).
3. C. Y. Yang *et al.*, *Phys. Rev. B* **36**, 8798 (1987); C. Y. Yang *et al.*, paper presented at 5th International Conference on X-Ray Absorption Fine Structure (University of Washington, Seattle, August 1988); J. B. Boyce *et al.*, *ibid.*; M. Qian *et al.*, *ibid.*
4. S. D. Conradson *et al.*, in preparation.
5. S. M. Heald, J. M. Tranquada, A. R. Moodenbaugh, Y. Xu, *Phys. Rev. B* **38**, 761 (1988).
6. N. Kosugi, H. Kondoh, H. Tajima, H. Kuroda, paper presented at 5th International Conference on X-Ray Absorption Fine Structure (University of Washington, Seattle, August 1988).
7. A. Bianconi *et al.*, *Phys. Rev. B* **26**, 6502 (1982); N. Kosugi, T. Yokoyama, H. Kuroda, *Chem. Phys.* **449**, 449 (1986).
8. T. A. Smith, J. E. Penner-Hahn, M. A. Berding, S. Doniach, K. O. Hodgson, *J. Am. Chem. Soc.* **107**, 5945 (1985).
9. L.-S. Kau, D. J. Spira-Solomon, J. E. Penner-Hahn, K. O. Hodgson, E. I. Solomon, *ibid.* **109**, 6433 (1987).
10. R. A. Bair and W. A. Goddard III, *Phys. Rev. B* **22**, 2767 (1980).
11. T. Yokoyama, N. Kosugi, H. Kuroda, *Chem. Phys.* **103**, 101 (1986).
12. As shown in (*8*) and (*9*), each particular transition to a localized state in copper K-edge XANES can shift by up to 3 to 4 eV as the coordination environment is altered. Assume that a minor phase is present at a concentration of 5%, which is already much larger than can occur in this sample. Then, because the XANES are normalized on a per atom basis, and using 0.5 as the absorbance of an individual transition, the 1% changes in the absorbance we observe represent 60% changes in the absorbance for the trace phase. We cannot envision any mechanism whereby this change in oscillator strength would not be accompanied by a large energy shift, especially for four separate transitions. The energy should actually be a better indicator of these kinds of changes than the intensity, but the limitations of the experiment are such that an absorbance difference of 1% or less can be measured whereas an energy shift of 0.2 eV is required to accomplish an observable change in the difference spectrum. At a realistic minor phase concentration of 1%, the changes in the absorbance of this phase would be 100% or greater, impossibly large.
13. S. D. Conradson, I. D. Raistrick, G. H. Kwei, in preparation.
14. J. J. Caponi *et al.*, *Europhys. Lett.* **3**, 1301 (1987).
15. M. A. Beno *et al.*, *Appl. Phys. Lett.* **51**, 57 (1987); W. I. F. David *et al.*, *Nature* **327**, 227 (1987); T. Siegrist *et al.*, *Phys. Rev. B* **35**, 7137 (1987); A. Williams *et al.*, *ibid.* **37**, 7960 (1988).
16. For the sake of consistency, we have adopted the same labels for the final states as in (*5*) and (*6*). Although we concur with the assignment of feature C to the Cu1 $4p_x\pi \leftarrow 1s$ transition, to a final state molecular orbital of π symmetry composed of the Cu1 $4p_x$ and O1 and O4 $(3)p_x$ atomic orbitals, we believe that feature D, assigned to the Cu2 $4p_z\pi \leftarrow 1s$ transition, actually involved a final state molecular orbital which is not strictly of π symmetry because it possesses at least some O4 $(3)p_z$ character, analogous to the Cu2 $3d_{z^2}$–O4 $2p_z$ band near the Fermi level. Another issue in these assignments is the choice of the single- or multi-electron model. In the multi-electron model (*10, 11*), used in the assignments for $YBa_2Cu_3O_7$ (*5, 6*), the final state of the C/D transition is the bound Cu $4p\pi$, and the lower energy A/B transition is assigned to the Cu $4p\pi$ + shakedown state. In the single-electron model (*8*), the final state of the C/D transition is the quasi-bound Cu $4p\pi$L (L = ligand), which differs from the lower energy A/B transition to the bound Cu $4p\pi$ final state in that it is more delocalized, with appreciable photoelectron density on ligand-centered orbitals. If the single-electron model is correct, because changes in the intensities of transitions are more significant than changes in their energies, the overlap is apparently affected more than the nature of the $4p\pi$L state. Therefore, our interpretation is based only on the fact that the final states of these transitions have Cu1 $4p_x$ and Cu2 $4p_z$ character, which has been observed experimentally (*5, 6*), and is independent of the exact nature of the final state.
17. R. J. Cava *et al.*, *Physica B* **153–155**, 560 (1988).
18. M. Mali *et al.*, *Phys. Lett. A* **124**, 112 (1987).
19. H. Oyanagi *et al.*, *Jpn. J. Appl. Phys.* **37**, L828 (1987); J. B. Boyce, F. Bridges, T. Claeson, R. S. Howland, T. H. Geballe, *Phys. Rev. B* **36**, 5251 (1987); E. D. Crozier, N. Alberding, K. R. Bauchspiess, A. J. Seary, S. Gygax, *Phys. Rev. B* **36**, 8288 (1987).
20. S. Massidda, J. Yu, A. J. Freeman, D. D. Koelling, *Phys. Lett. A* **122**, 198 (1987); J. Yu, S. Massidda, A. J. Freeman, D. D. Koelling, *ibid.*, p. 203.
21. H. Krakauer, W. E. Pickett, R. E. Cohen, *J. Supercon.* **1**, 111 (1988).
22. T. Laegreid, K. Fossheim, F. Fassenden, *Physica C* **153–155**, 1096 (1988); V. Mueller *et al.*, *ibid.*, p. 280; G. Canelli *et al.*, *ibid.*, p. 298.
23. U. Murek, J. Röhler, K. Keulerz, *ibid.*, p. 270; S. Della Longa *et al.*, paper presented at 5th International Conference on X-Ray Absorption Fine Structure (University of Washington, Seattle, August 1988).
24. R. A. Butera, *Phys. Rev. B* **37**, 5909 (1988); M. Ishikawa *et al.*, *Solid State Commun.* **66**, 201 (1988).
25. E. Braun, G. Jackel, B. Roden, J. G. Sereni, D. Wohlleben, *Z. Phys. B* **72**, 169 (1988); M. Lang *et al.*, *Europhys. Lett.* **4**, 1145 (1987); M. Francois *et al.*, *Physica C* **153–155**, 962 (1988).
26. C. Taliani *et al.*, *Solid State Commun.* **66**, 487 (1988).
27. N. Nücker, J. Fink, J. C. Fuggle, P. J. Durham, W. M. Temmerman, *Phys. Rev. B* **37**, 5158 (1988).
28. A. Bianconi *et al.*, paper presented at 5th International Conference on X-Ray Absorption Fine Structure (University of Washington, Seattle, August 1988).
29. N. M. Plakida *et al.*, *Europhys. Lett.* **4**, 1309 (1987).
30. C. M. Varma, S. Schmitt-Rink, E. Abrahams, *Solid State Commun.* **62**, 681 (1987).
31. J. E. Hirsch, S. Tang, E. Loh, Jr., D. J. Scalapino, *Phys. Rev. Lett.* **60**, 1668 (1988).
32. Z. Tesanovic, A. R. Bishop, R. L. Martin, *Solid State Commun.* **68**, 337 (1988).
33. W. A. Little, *Science* **242**, 1390 (1988).
34. ———, *Phys. Rev.* **134**, A1416 (1964).
35. E. Garcia *et al.*, *Phys. Rev. B* **38**, 2900 (1988).

36. We thank C. Ponader, G. Kwei, M. Zietlow, S. Ekberg, and the Stanford Synchrotron Radiation Laboratory (SSRL) operations staff for their assistance in acquiring these data, J. D. Thompson for the magnetic susceptibility measurements, and R. Albers, R. Martin, J. Wilkins, A. Bishop, Z. Fisk, and D. Smith for useful discussions and for reviewing this manuscript, as well as R. Scott for the XAFPAK data analysis software. Data acquisition and some analysis were done at SSRL, which is funded by the U.S. Department of Energy under contract DE-AC03-82ER-13000, Office of Basic Energy Sciences, Division of Chemical Sciences and the NIH Biotechnology Resource Program, Division of Research Resources. This work was supported by the Department of Energy via the Institutional Supporting Research Program and the Center for Materials Science at Los Alamos National Laboratory.

22 November 1988; accepted 24 January 1989

Honeyguides and Honey Gatherers: Interspecific Communication in a Symbiotic Relationship

H. A. ISACK AND H.-U. REYER*

In many parts of Africa, people searching for honey are led to bees' nests by the greater honeyguide (*Indicator indicator* Sparrman). The Boran people of Kenya claim that they can deduce the direction and the distance to the nest as well as their own arrival at the nest from the bird's flight pattern, perching height, and calls. Analyses of the behavior of guiding birds confirmed these claims.

ACCORDING TO ROCK PAINTINGS from the central Sahara, Zimbabwe, and South Africa, man has collected honey in Africa for 20,000 years (*1, 2*). Even today, honey contributes significantly to the diets of many African people (*2–5*). When searching for honey, Africans are often joined by the greater honeyguide (*Indicator indicator*), which leads them to bee colonies (*Apis mellifira*) located in large trees, rock crevices, or termite mounds. After the gatherers have opened and left the nest, the bird feeds on pieces of honeycomb left behind. From these it extracts mainly the larvae and the wax to supplement its normal diet of insects (*5–7*). The earliest written accounts of this bird-man interaction date back to the 17th century (*6*). Because of the anecdotal nature of most of these reports, however,

H. A. Isack, Department of Ornithology, National Museum of Kenya. Post Office Box 40658, Nairobi, Kenya. H.-U. Reyer, Max-Planck-Institut für Verhaltensphysiologie, D-8131 Seewiesen, Federal Republic of Germany.

*Present address and address for reprint requests: Zoologisches Institut der Universität Zürich, Winterthurerstrasse 190, CH-8057 Zürich, Switzerland.